

# Resonance $a_1(1420)$ and the Three-Pion Decays of the Tauon

Peter Lichard

*Institute of Physics, Silesian University in Opava,  
746 01 Opava, Czech Republic*

and

*Institute of Experimental and Applied Physics,  
Czech Technical University in Prague,  
128 00 Prague, Czech Republic*

The role of the  $a_1(1420)$  resonance in the three-pion decays of the  $\tau$  lepton is investigated using a phenomenological model. For all data before 2008, roughly equal fit quality is achieved when the basic  $a_1(1260)$  resonance is supplemented with either  $a_1(1640)$  or  $a_1(1420)$ . However, two recent and more precise data sets require resonances with masses that are not very far from that of  $a_1(1420)$ . This suggests that the axial-vector resonance that accompanies the  $a_1(1260)$  in the three-pion decays of the tauon is  $a_1(1420)$ , not  $a_1(1640)$ , as believed up to now. More data are needed to demonstrate this definitely.

Recently, I have compared our model [1] of the three-pion decays of the  $\tau$  lepton to nineteen experimental data sets found in literature from 1986 to 2013. A detailed account will be presented elsewhere [2].

In this Letter I report on one interesting byproduct of my study that is related to the  $a_1(1420)$  resonance, which was discovered in 2013 by the COMPASS Collaboration at CERN [3]. They performed a careful partial wave analysis of the  $\pi^-\pi^-\pi^+$  system produced in diffractive dissociation of 190 GeV/c pions off a stationary hydrogen target and then used the resonance-model fit to the spin density matrix to find the resonance parameters.

I first recapitulate the main features of our model [1]. Its physical content is depicted by the meson dominance [4] diagrams in Figs. 1 and 2.

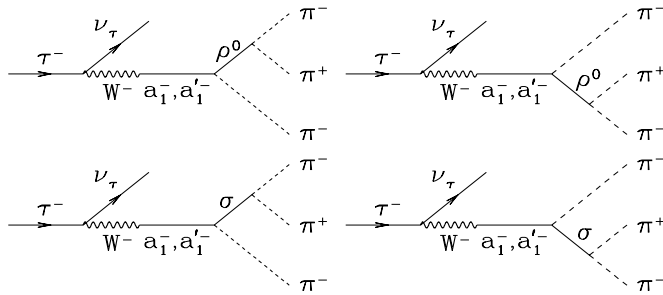


FIG. 1. Feynman diagrams of the  $\tau^- \rightarrow \nu_\tau \pi^-\pi^+\pi^-$  decay.

The interaction among the  $a_1(1260)$  (denoted simply as  $a_1$  in what follows),  $\rho$  and  $\pi$  fields is described by a two-component Lagrangian

$$\mathcal{L}_{a_1\rho\pi} = \frac{g_{a_1\rho\pi}}{\sqrt{2}} (\mathcal{L}_1 \cos \theta + \mathcal{L}_2 \sin \theta), \quad (1)$$

where  $\mathcal{L}_1 = \mathbf{A}^\mu \cdot (\mathbf{V}_{\mu\nu} \times \partial^\nu \mathbf{P})$ ,  $\mathcal{L}_2 = \mathbf{V}_{\mu\nu} \cdot (\partial^\mu \mathbf{A}^\nu \times \mathbf{P})$ , and  $\mathbf{V}_{\mu\nu} = \partial_\mu \mathbf{V}_\nu - \partial_\nu \mathbf{V}_\mu$ . The isovectors  $\mathbf{A}^\mu$ ,  $\mathbf{V}_\mu$ , and  $\mathbf{P}$  denote the operators of the  $a_1$ ,  $\rho$  and  $\pi$  fields, respectively. Although one can find several flaws in this Lagrangian from the QCD point of view, its soundness

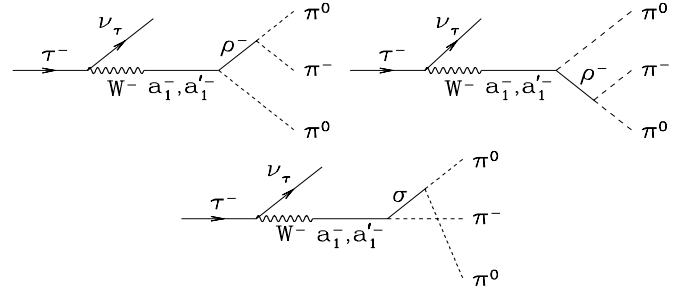


FIG. 2. Feynman diagrams of the  $\tau^- \rightarrow \nu_\tau \pi^-\pi^0\pi^0$  decay.

for low-energy phenomenology is supported by the fact that the same Lagrangian provided a good description of the four-pion production in the  $e^+e^-$  annihilation [5], even for the same value of the mixing parameter  $\sin \theta$ , as shown in [1].

The  $a_1$  propagator

$$-iG_{a_1}^{\mu\nu}(p) = \frac{-g^{\mu\nu} + p^\mu p^\nu / m_{a_1}^2}{s - M_{a_1}^2(s) + im_{a_1} \Gamma_{a_1}(s)} \quad (2)$$

features running mass  $M_{a_1}(s)$  given by a once-subtracted dispersion relation with the energy-dependent total width  $\Gamma_{a_1}(s)$  as input. The following contributions to  $\Gamma_{a_1}(s)$  are considered:  $a_1 \rightarrow \rho + \pi \rightarrow 3\pi$ ,  $a_1 \rightarrow \bar{K}^*K, K^*\bar{K} \rightarrow K\bar{K}\pi$ , and  $a_1 \rightarrow \sigma + \pi \rightarrow 3\pi$  and the following conditions are satisfied:  $M_{a_1}^2(m_{a_1}^2) = m_{a_1}^2$ ,  $\Gamma_{a_1}(m_{a_1}^2) = \Gamma_{a_1}$ .

When an additional axial-vector resonance  $a_1'$  is included, the same Lagrangian (1) is used with the same mixing parameter  $\sin \theta$ . Instead of (2), a simpler  $a_1'$  propagator is chosen, with running mass replaced by the nominal  $a_1'$  mass and with the energy dependent total width given by  $\Gamma_{a_1'}(s) = k\Gamma_{a_1}(s)$ , with constant  $k$  guaranteeing that the condition  $\Gamma_{a_1'}(m_{a_1'}^2) = \Gamma_{a_1'}$  is fulfilled.

The propagator of the  $\rho(770)$  resonance is taken in a variable-width, running-mass form [6].

The interaction Lagrangian among the  $a_1$ ,  $\pi$ , and  $\sigma$

fields is written in the form

$$\mathcal{L}_{a_1\sigma\pi} = g_1 (\mathbf{A}^\mu \cdot \partial_\mu \mathbf{P}) S + g_2 (\mathbf{A}^\mu \cdot \mathbf{P}) \partial_\mu S, \quad (3)$$

where  $S$  is the operator of the  $\sigma$  field. For the  $\sigma$  propagator we use a simple form with the fixed mass and energy dependent width.

All strong interaction vertexes are modified by the form factor  $F(q) = \exp\{-q^2/(12\beta^2)\}$ , where  $q$  is the three-momentum magnitude of a daughter meson in the rest frame of the parent meson. It is taken from the chromoelectric flux-tube breaking model of Kokoski and Isgur [7], together with their value  $\beta = 0.4 \text{ GeV}/c$ .

The model without  $a'_1$  contains six adjustable parameters: (i) a multiplicative constant ensuring the correct normalization to the data, which absorbs the product of all coupling constants from the  $a_1 \rightarrow \rho$  branch, (ii)  $a_1$  mass, (iii)  $a_1$  width, (iv)  $a_1\rho\pi$  Lagrangian mixing parameter  $\sin\theta$ , (v-vi) two different products of the coupling constants from the  $a_1 \rightarrow \sigma$  branch scaled by the product of coupling constants from the  $a_1 \rightarrow \rho$  branch.

If an  $a'_1$  is included, a complex constant enters, which multiplies the  $a'_1$  propagator before adding it to the  $a_1$  propagator. The number of adjustable parameters is thus eight. If the mass and width of  $a'_1$  are allowed to vary, then the number of adjustable parameters rises to ten. Finally, if a combined set of  $N$  individual data sets is fitted, then the number of adjustable parameters increases by  $N-1$  because every data set requires its own normalization constant.

When we were completing our model [1], the existing data on the three-pion decays of the tauon were not precise enough to consider the  $a_1(1640)$  mass and width as free parameters. Therefore, we used their values from the 2008 Review of Particle Physics [8], which are still used today. As I will show, the situation has changed with the advent of two more precise sets of data. The first, which appeared in the PhD Thesis of I. M. Nugent [9], published in 2009, may be regarded as a very preliminary version of the BaBar data [10]. The other set contains very precise data from the Belle Collaboration at the KEKB collider, published in 2010 [11].

An important indicator of the soundness of our model is that the parameters required for a good fit to various data sets are very similar. It is therefore possible to obtain a satisfactory fit for several data sets combined together, as shown in [1].

The original model [1] has been slightly modified: (i) the bin width in the modified ALEPH data [12] varies from point to point in the high mass part of the spectrum, which required a corresponding change in the software; (ii) following the advice of Dr. David Bugg [13], I introduced an option to mimic the Adler zero [14] in the  $\sigma \rightarrow \pi + \pi$  amplitude; (iii) in the original model [1], one of the two  $a_1\sigma\pi$  coupling constants was fixed by requiring the vanishing derivative of the  $a_1$  running mass at the resonance point. I have released this connection

and introduced another free parameter (already included in the list above).

After I learned of the discovery of the  $a_1(1420)$  resonance by the COMPASS Collaboration [3], I made all the calculations with both options, namely with  $a'_1 \equiv a_1(1640)$  and  $a'_1 \equiv a_1(1420)$ . The results presented here were evaluated with the  $a_1(1420)$  mass of 1411.8 MeV and width of 158 MeV in accordance with a recent COMPASS submission to arXiv [15].

Concerning the influence of the presence or choice of a particular  $a'_1$  on the agreement of our model with data, the experimental data can be divided into three categories.

In the first category, there are four data sets [16] (CELLO 90c [17], CELLO 90m [17], Nugent 09c [9], Belle 10c [11]) which our model is not able to describe (confidence level, C.L., was less than 10%) whether the  $a'_1$  is included or not.

Then, there is a group of eight data sets (Argus 93c [18], OPAL 95c [19], OPAL 97c [20], ALEPH 98m [21], OPAL 99c [22], OPAL 99m [22], ALEPH 05m [23], ALEPH 13m [12]), five of them with C.L. of 100%, with which our model agrees, even if the  $a'_1$  is not considered.

The last category includes seven experiments (Mark II 86c [24], MAC 87c [25], MAC 87m [25], ALEPH 98c [21], CLEO 00m [26], ALEPH 05c [23], ALEPH 13c [12]) in which the inclusion of the  $a'_1$  in the model improves its agreement with data (for three of them, the C.L. then reached more than 98%). The quality of the fit depends only marginally on the  $a'_1$  species.

The examples of data sets from each category are shown in Table I. The results of five selected individual data sets are accompanied by the result of a simultaneous fit to six data sets (ARGUS 93c, OPAL 99c, OPAL 99m, CLEO 00m, ALEPH 05c, ALEPH 05m), which is denoted as Set A. The first two lines (Set A and ALEPH 13m) show examples of a good fit achieved without the help of  $a_1(1640)$  or  $a_1(1420)$ . If either of them is included, the  $\chi^2$  decreases, but there is no influence on the already perfect confidence level.

Sets ALEPH 05c and ALEPH 13c are examples of data that are fitted better when any  $a'_1$  is included. For ALEPH 13c, the confidence level rose from 0.3 to 21.7 per cent [20.1 per cent] if  $a_1(1640)$  [ $a_1(1420)$ ] is chosen. For ALEPH 05c, confidence level even reaches 100 per cent for either choice. The last two rows show that our model is unable to fit Nugent 09c and Belle 10c data even if  $a'_1$  is considered.

In any case, it is encouraging that with the Nugent 09c data, replacing the  $a_1(1640)$  with  $a_1(1420)$  leads to a dramatic drop in the  $\chi^2$  and some increase in the confidence level, from  $\chi^2/\text{NDF} = 194.1/57$  (C.L.=0%) to  $\chi^2/\text{NDF} = 78.8/57$  (C.L.=2.9%). This has prompted me to allow both the  $a'_1$  mass and width vary. As a result, the confidence level climbs to 100%, based on  $\chi^2/\text{NDF} = 18.7/55$ . Corresponding values of the  $a'_1$  mass and width

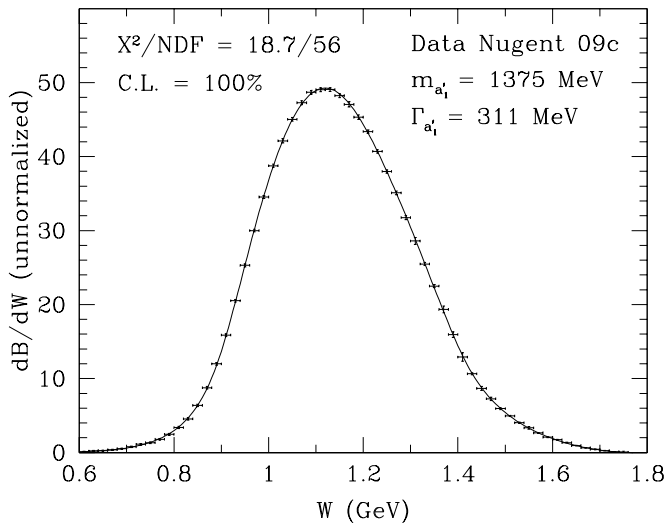


FIG. 3. Differential branching fraction in the invariant mass of the  $\pi^- \pi^+ \pi^-$  system. Comparison of the model with the Nugent 09c data [9].

are shown in Table II, together with their Minit [27] errors. A comparison of the experimental and calculated three-pion mass spectra appears in Fig. 3.

Repeating the procedure with the Belle 10c data, I have again achieved a very good fit (C.L.=95.5%) for the parameters displayed in Table II. The  $a'_1$  mass is almost identical to that of the Nugent 09c data; though the width is higher. The model curve goes perfectly through the experimental points, which have very small errors. See Fig. 4.

It may seem disturbing that the resonances that have been found in the Nugent 09c and Belle 10c data by minimizing  $\chi^2$  are not visible in Figs. 3 and 4 as bumps or shoulders. The reason is that the interference between the  $a_1(1260)$  and  $a'_1$  is destructive, as discussed in [1]. See Figs. 5 and 6 there.

The situation with the ALEPH 13c data is special. An attempt to obtain the optimal  $a'_1$  parameters by minimizing  $\chi^2$  was unsuccessful. The minimization procedure strayed into an unphysical region. But when the  $a'_1$  parameters extracted from the Nugent 09c or Belle 10c data shown in Table II were used, the resulting confidence level became much better than that with the  $a_1(1640)$  or  $a_1(1420)$ . Compare Table III with ALEPH 13c row in Table I.

It is tempting to assume that the resonance extracted from the Nugent 09c and Belle 10c data, which is also preferred by the ALEPH 13c data, is identical to the resonance  $a_1(1420)$  observed by the COMPASS Collaboration. It would be surprising to have two different resonances so close in mass.

However, when we consult Table II and compare the parameters of the  $a'_1$  resonance from the study of the three-pion decays of the tauon with those found by the

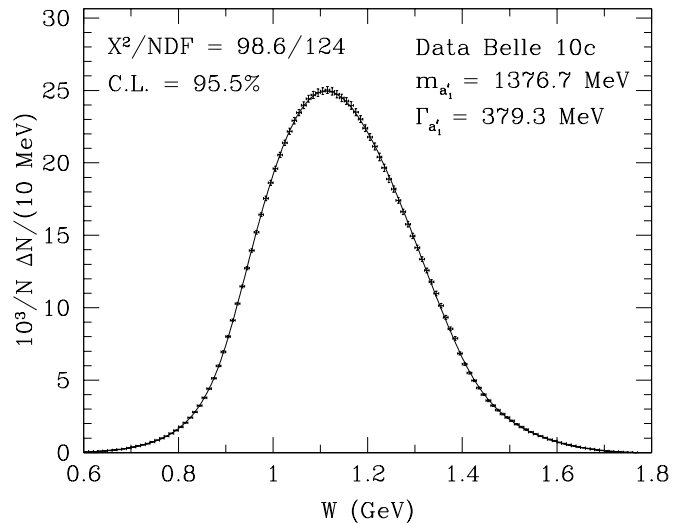


FIG. 4. Three-pion mass spectrum measured by the Belle Collaboration [11] fitted by our model.

COMPASS Collaboration, we find a serious discrepancy in the decay widths. The  $a_1(1420)$  decay width is about half of those from the Nugent 09c and Belle 10c data. A possible reason for this discrepancy may be a different parametrization of the resonance width. The COMPASS Collaboration used the width modified by the Blatt–Weisskopf centrifugal-barrier factors in their relativistic Breit–Wigner formulas [28]. On the other hand, in our model the  $a'_1$  width is obtained by rescaling the width of  $a_1(1260)$ .

The COMPASS Collaboration has shown that the  $a_1(1420)$  decays into pion and  $f_0(980)$ . The main drawback of our model is that we consider the  $\sigma \equiv f_0(500)$  instead. However, at this stage, it does not make much sense to begin a labor intensive modification of our model by allowing different scalar resonances for  $a_1(1260)$  and  $a_1(1420)$ . Our model in its present form shows perfect agreement with both the Nugent 09c and Belle 10c data. Clearly, more data are needed that would falsify our model and force it to discriminate between the  $\sigma$  and  $f_0(980)$ .

To conclude, the phenomenological analysis of the Nugent [9] and Belle [11] data offers a serious hint that the excited axial-vector resonance which plays a role in the three-pion decays of the tauon is the  $a_1(1420)$ , not  $a_1(1640)$ .

Earlier collaboration with Dr. Martin Vojík is gratefully acknowledged. Martin independently coded the model [1] in C++ programming language, and by reaching the same results as from my Fortran code, provided an important test of the software. Thanks also to Drs. Mikihiro Nakao (for Belle spokespersons) and MyeongJae Lee for promptly providing the Belle data, to Dr. David Bugg for valuable correspondence, and to Dr. Josef Juráň for discussions. This work was partly supported by the

Czech MSMT projects Inter-Excellence No. LTT17018 and INGO II No. LG15052.

- 
- [1] M. Vojík and P. Lichard, arXiv: 1006.2919 [hep-ph].
- [2] P. Lichard, in preparation.
- [3] S. Paul (for the COMPASS Collaboration) EPJ Web Conf. **73**, 03002 (2014); C. Adolph *et al.* (COMPASS Collaboration), Phys. Rev. Lett. **115**, 082001 (2015); Phys. Rev. D **95**, 032004 (2017).
- [4] P. Lichard, Phys. Rev. D **55**, 5385 (1997).
- [5] P. Lichard and J. Juráň, Phys. Rev. D **76**, 094030 (2007); J. Juráň and P. Lichard, *ibid.* **78**, 017501 (2008).
- [6] P. Lichard, Phys. Rev. D **60**, 053007 (1999); M. Vojík and P. Lichard, arXiv:hep-ph/0611163.
- [7] R. Kokoski and N. Isgur, Phys. Rev. D **35**, 907 (1987).
- [8] C. Amsler *et al.* (Particle Data Group), Phys. Lett. B **667**, 1 (2008)
- [9] I. M. Nugent, PhD Thesis. SLAC-R-936 (2009).
- [10] Later, at least two other versions of the BaBar preliminary data were mentioned in literature [29, 30], but no final publication and/or data table is available yet.
- [11] M. J. Lee *et al.* (Belle Collaboration), Phys. Rev. D **81**, 113007 (2010).
- [12] M. Davier, A. Höcker, B. Malaescu, C. Z. Yuan, Z. Zhang, Eur. Phys. J. C **74**, 2803 (2014).
- [13] D. Bugg, private communication.
- [14] S. L. Adler, Phys. Rev. **137**, B1022 (1965).
- [15] F. Krinner (for the COMPASS Collaboration), arXiv: 1611.01388 [hep-ex].
- [16] I use the letters *c* and *m* to distinguish between the  $\pi^-\pi^+\pi^-$  (charged) and  $\pi^-\pi^0\pi^0$  (mixed) three pion systems.
- [17] H. J. Behrend *et al.* (CELLO Collaboration), Z. Phys. C **46**, 537 (1990).
- [18] H. Albrecht *et al.* (ARGUS Collaboration), Z. Phys. C **58**, 61 (1993).
- [19] R. Akers *et al.* (OPAL Collaboration), Z. Phys. C **67**, 45 (1995)
- [20] K. Ackerstaff *et al.* (OPAL Collaboration), Z. Phys. C **75**, 593 (1997).
- [21] R. Barate *et al.* (ALEPH Collaboration), Eur. Phys. J. C **4**, 409 (1998).
- [22] K. Ackerstaff *et al.* (OPAL Collaboration), Eur. Phys. J. C **7**, 571 (1999).
- [23] S. Schael *et al.* (ALEPH Collaboration), Physics Reports **421**, 191 (2005).
- [24] W. B. Schmidke *et al.*, Phys. Rev. Lett. **57**, 527 (1986).
- [25] H. R. Band *et al.* (MAC Collaboration), Phys. Lett. B **198**, 297 (1987).
- [26] D. M. Asner *et al.* (CLEO Collaboration), Phys. Rev. D **61**, 012002 (2000); arXiv: hep-ex/9902022.
- [27] F. James and M. Roos, Comput. Phys. Commun. **10**, 343 (1975).
- [28] F. Haas, Report No. CERN-THESIS-2013-277.
- [29] I. M. Nugent (on behalf of the BaBar Collaboration), Nucl. Phys. B (Proc. Suppl.) **253-255**, 38 (2014).
- [30] I. M. Nugent *et al.*, Phys. Rev. D **88**, 093012 (2013).

TABLE I. Confidence level (C.L.) of the fits to various data assuming various axial-vector recurrences  $a'_1$ . Usual  $\chi^2$  and the number of degrees of freedom (NDF) are also shown.

Data	$\chi^2$	No $a'_1$		$a'_1 \equiv a_1(1640)$			$a'_1 \equiv a_1(1420)$		
		NDF	C.L.(%)	$\chi^2$	NDF	C.L.(%)	$\chi^2$	NDF	C.L.(%)
Set A	368.0	462	100.0	267.1	460	100.0	300.6	460	100.0
ALEPH 13m	31.2	68	100.0	30.3	66	100.0	30.5	66	100.0
ALEPH 05c	102.9	110	67.0	23.7	108	100.0	45.2	108	100.0
ALEPH 13c	103.6	67	0.3	73.6	65	21.7	74.3	65	20.1
Nugent 09c	552.8	59	0.0	194.1	57	0.0	78.8	57	2.9
Belle 10c	1607.1	126	0.0	845.4	126	0.0	572.5	126	0.0

TABLE II. Searching for the  $a'_1$  parameters. Only errors coming from Minuit [27] are shown, no attempt to estimate the systematic errors of the model has been made. Also the COMPASS [3] results are shown for comparison.

Data	$m$ (MeV)	$\Gamma$ (MeV)	$\chi^2$	NDF	C.L.(%)
Nugent 09c	$1375 \pm 11$	$311 \pm 8$	18.7	56	100.0
Belle 10c	$1376.7 \pm 1.2$	$379.3 \pm 6.3$	98.6	124	95.5
COMPASS	$1414^{+15}_{-13}$	$153^{+8}_{-23}$			

TABLE III. Fit to the ALEPH 13c [12] data assuming the  $a'_1$  parameters found from the Nugent 09c and Belle 10c data.

	$\chi^2$	NDF	C.L.(%)
$a'_1$ from Nugent 09c	65.1	65	47.3
$a'_1$ from Belle 10c	65.9	65	44.6